International Journal of Scientific Engineering and Science
Volume 9, Issue 12, pp. 66-75, 2025. ISSN (Online): 2456-7361

Efficient Spectral Galerkin Method Based on a Mixed Scheme for Fourth-Order Problems in Ellipsoidal Domain

Jihui Zheng[1,*], Wei Wang[1]
[1]School of Mathematics Science, Guizhou Normal University, Guiyang 550025, China

Abstract— *In this paper, we propose and analysis a computationally efficient mixed spectral Galerkin method for solving fourth-order problems in ellipsoidal domain. The approach begins by reformulating the fourth-order equation as a coupled system of second-order equations. A novel spherical coordinate transformation is then introduced, mapping the ellipsoidal domain onto the unit sphere to enable spectral discretization. Building on this transformation, we derive a mixed variational formulation and its discrete scheme. Finally, numerical experiments validate the algorithm's efficacy and spectral accuracy.*

Keywords— *Fourth-order problems; mixed scheme; spectral-Galerkin method; ellipsoidal domain.*

I. Introduction

Spectral methods are widely recognized for providing highly accurate approximations with relatively few degrees of freedom, and have been extensively studied and applied in scientific computation [1, 2, 3, 4, 5, 6, 7, 8]. However, their application has been predominantly limited to regular domains such as cubes, spheres, and rectangles. For complex geometries, domain decomposition and spectral element methods have been developed [9, 10, 11, 12, 13, 14, 15], which partition an irregular domain into regular subdomains. Although effective for polygonal regions, these methods are generally not well-suited for maintaining high-order accuracy on irregular curved domains.

For PDEs on curved geometries, established numerical approaches include finite differences [16], spectral methods [17, 18], and finite element methods [19, 20, 21, 22]. While FEM can handle irregular surfaces, it typically requires surface discretization and approximation of geometric differential operators, which introduces additional complexity. Developing direct spectral methods for curved geometries therefore remains an area of significant interest. Current strategies often employ an embedding technique [23] or a mapping approach that transforms the curved domain onto a regular one via an explicit smooth mapping [24] or a Gordon-Hall type mapping [25]. Related works include spectral embedding methods for PDEs in curved geometries [26], well-posed fictitious domain spectral methods for elliptic problems [27, 28], and spectral methods based on coordinate transformations for two-dimensional curved domains [24, 29].

Despite these advances, PDEs in three-dimensional curved geometries are of critical importance in science and engineering, yet direct spectral methods for such 3D problems remain scarce. Some notable efforts include a Fourier-Legendre spectral-Galerkin method for second-order PDEs in general 3D curved domains [30], and an embedding approach that immerses a 3D domain into a larger sphere [28]. Nonetheless, efficient and high-order spectral methods tailored for specific 3D curved regions are still highly desirable.

In this paper, we focus on the three-dimensional ellipsoidal domain and develop an efficient mixed spectral-Galerkin scheme for fourth-order problems. Our approach consists of three main steps: (i) reformulating the fourth-order equation into a coupled second-order system; (ii) introducing a specialized spherical coordinate transformation that maps the ellipsoid onto the unit sphere; and (iii) deriving a mixed variational formulation and its discrete spectral approximation. To validate the proposed algorithm, we perform extensive numerical tests, which confirm its efficacy and high-order accuracy.

The remainder of this paper is organized as follows. In section 2, we deduce the equivalent coupled system and its mixed variational form. In section 3, we provide a detailed description of the effective implementation process of the algorithm. In section 4, we con-duct several numerical tests. Finally, we make a conclusion comment in Section 5.

II. Equivalent coupled system and its mixed variational form

We initially consider the following fourth-order eigenvalue problem as a model case:

$$\begin{aligned} &\Delta^2\psi(\mathbf{x}) - \alpha\Delta\psi(\mathbf{x}) + \beta\psi(\mathbf{x}) = \lambda\psi(\mathbf{x}), && \mathbf{x}\in\Omega, \\ &\psi(\mathbf{x}) = 0, \Delta\psi(\mathbf{x}) = 0, && \mathbf{x}\in\partial\Omega, \end{aligned} \qquad (1)$$

where α and β are non-negative constants, and $\Omega \subset \mathbb{R}^3$ is an ellipsoidal domain.

We now introduce an auxiliary equation $\phi(\mathbf{x}) = -\Delta\psi(\mathbf{x})$. Then, (1) can be restated as follows:

Volume 9, Issue 12, pp. 66-75, 2025. ISSN (Online): 2456-7361

$$\begin{aligned} &-\Delta\phi(\mathbf{x})+\alpha\phi+\psi=\hat{\lambda}\psi(\mathbf{x}), && \mathbf{x}\in\Omega,\\ &-\Delta\psi-\phi=0, && \mathbf{x}\in\Omega, \quad (2)\\ &\psi(\mathbf{x})=0,\phi(\mathbf{x})=0, && \mathbf{x}\in\partial\Omega, \end{aligned}$$

where $\hat{\lambda}=\lambda-\beta+1$.

Let $H^s(\Omega)$ denote the Sobolev space of order s, with $\|\cdot\|_s$ and $|\cdot|_s$ representing its associated norm and semi-norm, respectively. Applying boundary conditions and Green's formula to (2), we derive the following mixed variational formulation: Find $[\phi,\psi]\in H_0^1(\Omega)\times H_0^1(\Omega)$ such that

$$\mathrm{G}\langle[\phi,\psi],[h,g]\rangle=\hat{\lambda}\Re\langle[\phi,\psi],[h,g]\rangle,[h,g]\in H_0^1(\Omega)\times H_0^1(\Omega), \tag{3}$$

where

$$\mathrm{G}\langle[\phi,\psi],[h,g]\rangle=\int_\Omega \nabla\phi\cdot\nabla h+\alpha\phi h+\psi h-\phi g+\nabla\psi\cdot\nabla g d\Omega,$$

$$\Re\langle[\phi,\psi],[h,g]\rangle=\int_\Omega \psi h d\Omega.$$

Building on [30], we define the spherical coordinate transformation:

$$\begin{cases} x=r\rho(\theta,\varphi)\cos\theta\sin\varphi, & r\in[0,1),\varphi\in[0,\pi],\theta\in[0,2\pi),\\ y=r\rho(\theta,\varphi)\sin\theta\sin\varphi, & r\in[0,1),\varphi\in[0,\pi],\theta\in[0,2\pi),\\ z=r\rho(\theta,\varphi)\cos\varphi, & r\in[0,1),\varphi\in[0,\pi], \end{cases} \tag{4}$$

where $\rho(\theta,\varphi)>0$ represents the distance from the origin to the surface S and depends solely on the latitude θ and longitude φ. Assume

$\partial_\varphi\rho(\theta,\varphi),\partial_\theta\rho(\theta,\varphi),\partial_\varphi\partial_\theta\rho(\theta,\varphi)\in L^\infty(\Xi),\Xi=[0,2\pi]\times[0,\pi].$

Let us denote

$$\sigma(\tau,\theta,\varsigma)=\phi(r\rho(\theta,\varphi)\cos\theta\sin\varphi,r\rho(\theta,\varphi)\sin\theta\sin\varphi,r\rho(\theta,\varphi)\cos\varphi),$$

$$\tilde{n}(\tau,\theta,\varsigma)=\psi(r\rho(\theta,\varphi)\cos\theta\sin\varphi,r\rho(\theta,\varphi)\sin\theta\sin\varphi,r\rho(\theta,\varphi)\cos\varphi),$$

$$r=\frac{\tau+1}{2},\varphi=\frac{\pi(\varsigma+1)}{2},(\tau,\theta,\varsigma)\in D=(-1,1)\times[0,2\pi)\times(-1,1).$$

Applying (4) through direct computation yields

$$\begin{aligned} \partial_x=&[\frac{\cos\theta}{\rho(\theta,\varphi)\sin\varphi}+\frac{\sin\theta}{\rho^2(\theta,\varphi)\sin\varphi}\partial_\theta\rho-\frac{\cos^2\varphi\cos\theta}{\rho(\theta,\varphi)\sin\varphi}-\frac{\cos\varphi\cos\theta}{\rho^2(\theta,\varphi)}\partial_\varphi\rho]\partial_r\\ &-\frac{\sin\theta}{r\rho(\theta,\varphi)\sin\varphi}\partial_\theta+\frac{\cos\varphi\cos\theta}{r\rho(\theta,\varphi)}\partial_\varphi,\\ \partial_y=&[\frac{\sin\theta}{\rho(\theta,\varphi)\sin\varphi}-\frac{\cos\theta}{\rho^2(\theta,\varphi)\sin\varphi}\partial_\theta\rho-\frac{\cos^2\varphi\sin\theta}{\rho(\theta,\varphi)\sin\varphi}-\frac{\cos\varphi\sin\theta}{\rho^2(\theta,\varphi)}\partial_\varphi\rho]\partial_r\\ &+\frac{\cos\theta}{r\rho(\theta,\varphi)\sin\varphi}\partial_\theta+\frac{\cos\varphi\sin\theta}{r\rho(\theta,\varphi)}\partial_\varphi,\\ \partial_z=&[\frac{\cos\varphi}{\rho(\theta,\varphi)}+\frac{\sin\varphi}{\rho^2(\theta,\varphi)}\partial_\varphi\rho(\theta,\varphi)]\partial_r-\frac{\sin\varphi}{r\rho(\theta,\varphi)}\partial_\varphi. \end{aligned} \tag{5}$$

This yields

International Journal of Scientific Engineering and Science
Volume 9, Issue 12, pp. 66-75, 2025. ISSN (Online): 2456-7361

$$\begin{aligned}\nabla\phi(x,y,z)=(\partial_x\phi,\partial_y\phi,\partial_z\phi)=2\Big(&\ [\frac{\cos\theta}{\rho\sin\varphi}+\frac{\sin\theta}{\rho^2\sin\varphi}\partial_\theta\rho-\frac{\cos^2\varphi\cos\theta}{\rho\sin\varphi}\\ &-\frac{\cos\varphi\cos\theta}{\rho^2}\partial_\varphi\rho]\partial_\tau\sigma-\frac{\sin\theta}{(\tau+1)\rho\sin\varphi}\partial_\theta\sigma+\frac{2\cos\varphi\cos\theta}{\pi(\tau+1)\rho}\partial_\varsigma\sigma,\\ &[\frac{\sin\theta}{\rho\sin\varphi}-\frac{\cos\theta}{\rho^2\sin\varphi}\partial_\theta\rho-\frac{\cos^2\varphi\sin\theta}{\rho\sin\varphi}-\frac{\cos\varphi\sin\theta}{\rho^2}\partial_\varphi\rho]\partial_\tau\sigma+\frac{\cos\theta}{(\tau+1)\rho\sin\varphi}\partial_\theta\sigma\\ &+\frac{2\cos\varphi\sin\theta}{\pi(\tau+1)\rho}\partial_\varsigma\sigma,[\frac{\cos\varphi}{\rho}+\frac{\sin\varphi}{\rho^2}\partial_\varphi\rho]\partial_\tau\sigma-\frac{2\sin\varphi}{\pi(\tau+1)\rho}\partial_\varsigma\sigma\ \Big).\end{aligned}\tag{6}$$

Based on equality (6), σ and ñ must satisfy the pole conditions:

$$\partial_\theta\sigma(\tau,\theta,-1)=\partial_\theta\sigma(\tau,\theta,1)=\partial_\theta\sigma(-1,\theta,\varsigma)=\partial_\varsigma\sigma(-1,\theta,\varsigma)=0,$$

$$\partial_\theta \tilde{n}(\tau,\theta,-1)=\partial_\theta \tilde{n}(\tau,\theta,1)=\partial_\theta \tilde{n}(-1,\theta,\varsigma)=\partial_\varsigma \tilde{n}(-1,\theta,\varsigma)=0.$$

We define two non-uniformly weighted Sobolev spaces:

$$L^2_{\omega,0}(D)=\left\{\sigma:\int_D\omega\rho^3(\theta,\varphi)\sin\varphi|\sigma|^2\,dD<\infty\right\},\text{ where }\omega=(1+\tau)^2,$$

$$\begin{aligned}V^1_{*,0}(D):=\Big\{\sigma:\int_D&\omega p(\theta,\varphi)|\partial_\tau\sigma|^2+\frac{\rho}{\sin\varphi}|\partial_\theta\sigma|^2+\rho\sin\varphi|\partial_\varsigma\sigma|^2\\ &-\Big[(1+\tau)\partial_\varphi\rho\sin\varphi\partial_\varsigma\sigma\partial_\tau\sigma+\frac{\pi(1+\tau)\partial_\theta\rho}{2\sin\varphi}\partial_\theta\sigma\partial_\tau\sigma\Big]\\ &+\omega\rho^3(\theta,\varphi)\sin\varphi|\sigma|^2\,dD<\infty,\sigma(\tau,\theta,\varsigma)=\sigma(\tau,2\pi+\theta,\varsigma),\sigma(1,\theta,\varsigma)=0,\\ &\partial_\theta\sigma(\tau,\theta,-1)=\partial_\theta\sigma(\tau,\theta,1)=\partial_\theta\sigma(-1,\theta,\varsigma)=\partial_\varsigma\sigma(-1,\theta,\varsigma)=0\Big\}\end{aligned}$$

with

$$p(\theta,\varphi)=\rho(\theta,\varphi)\sin\varphi+\frac{\sin\varphi[\partial_\varphi\rho(\theta,\varphi)]^2}{\rho(\theta,\varphi)}+\frac{[\partial_\theta\rho(\theta,\varphi)]^2}{\rho(\theta,\varphi)\sin\varphi},$$

endowed with inner products and norms defined respectively as

$$(\sigma,\upsilon)_{\omega,0}=\int_D\omega\rho^3(\theta,\varphi)\sin\varphi\sigma\upsilon dD,\|\sigma\|_{\omega,0}=\Big(\int_D\omega\rho^3(\theta,\varphi)\sin\varphi|\sigma|^2\,d\tau d\theta d\varsigma\Big)^{\frac{1}{2}},$$

$$\begin{aligned}(\sigma,\upsilon)_{1,*,0}=\int_D&\omega p(\theta,\varphi)\partial_\tau\sigma\partial_\tau\upsilon+\frac{\rho(\theta,\varphi)}{\sin\varphi}\partial_\theta\sigma\partial_\theta\upsilon+\rho(\theta,\varphi)\sin\varphi\partial_\varsigma\sigma\partial_\varsigma\upsilon\\ &-\Big[\frac{1+\tau}{2}\partial_\varphi\rho\sin\varphi(\partial_\varsigma\sigma\partial_\tau\upsilon+\partial_\tau\sigma\partial_\varsigma\upsilon)+\frac{\pi(1+\tau)\partial_\theta\rho(\theta,\varphi)}{4\sin\varphi}(\partial_\theta\sigma\partial_\tau\upsilon+\partial_\tau\sigma\partial_\theta\upsilon)\Big]\\ &+\omega\rho^3(\theta,\varphi)\sin\varphi\sigma\upsilon dD,\|\sigma\|_{1,*,0}=[(\sigma,\sigma)_{1,*,0}]^{\frac{1}{2}}.\end{aligned}$$

We now define the product-type Sobolev spaces:

$$\overset{0}{\mathbf{V}}_{\mathring{a}}(D):=L^2_{\omega,0}(D)\times L^2_{\omega,0}(D),\qquad \overset{1}{\mathbf{V}}_{\mathring{a}}(D):=V^1_{*,0}(D)\times V^1_{*,0}(D),$$

and the corresponding norms are given by

$$\|[\hat{w},\hat{u}]\|_{\omega,D}=(\|\hat{w}\|^2_{\omega,0}+\|\hat{u}\|^2_{\omega,0})^{\frac{1}{2}},\|[\hat{w},\hat{u}]\|_{1,\mathring{a},D}=(\|\hat{w}\|^2_{1,*,0}+\|\hat{u}\|^2_{1,*,0})^{\frac{1}{2}}.$$

Subsequently, the weak formulation (3) is recast as: Find $\hat{\lambda}\in\square$ and nontrivial $[\sigma,\tilde{n}]\in\overset{1}{\mathbf{V}}_{\mathring{a}}(D)$ such that

$$\mathrm{A}\langle[\sigma,\tilde{n}],[\upsilon,\chi]\rangle=\hat{\lambda}\mathrm{B}\langle[\sigma,\tilde{n}],[\upsilon,\chi]\rangle,[\upsilon,\chi]\in\overset{1}{\mathbf{V}}_{\mathring{a}}(D),\tag{7}$$

where

$$\mathrm{A}\langle[\sigma,\tilde{n}],[\upsilon,\chi]\rangle=\int_D \frac{\pi}{4}\omega p(\theta,\varphi)\partial_\tau\sigma\partial_\tau\upsilon+\frac{\pi\rho}{4\sin\varphi}\partial_\theta\sigma\partial_\theta\upsilon+\frac{1}{\pi}\rho\sin\varphi\partial_\varsigma\sigma\partial_\varsigma\upsilon$$
$$+\frac{\alpha\pi}{16}\omega\rho^3\sin\varphi\sigma\upsilon-\frac{\tau+1}{\pi}\sin\varphi\partial_\varphi\rho(\partial_\varsigma\sigma\partial_\tau\upsilon+\partial_\tau\sigma\partial_\varsigma\upsilon)+\frac{\pi}{16}\omega\rho^3\sin\varphi\tilde{n}\upsilon$$
$$-\frac{\pi(\tau+1)\partial_\theta\rho}{4\sin\varphi}(\partial_\theta\sigma\partial_\tau\upsilon+\partial_\tau\sigma\partial_\theta\upsilon)-\frac{\pi}{16}\omega\rho^3\sin\varphi\sigma\chi$$
$$+\{\frac{\pi}{4}\omega p(\theta,\varphi)\partial_\tau\tilde{n}\partial_\tau\chi+\frac{\pi\rho}{4\sin\varphi}\partial_\theta\tilde{n}\partial_\theta\chi+\frac{1}{\pi}\rho\sin\varphi\partial_\varsigma\tilde{n}\partial_\varsigma\chi$$
$$-\frac{\tau+1}{\pi}\sin\varphi\partial_\varsigma\rho(\partial_\varsigma\tilde{n}\partial_\tau\chi+\partial_\tau\tilde{n}\partial_\varsigma\chi)-\frac{\pi(\tau+1)\partial_\theta\rho}{4\sin\varphi}(\partial_\theta\tilde{n}\partial_\tau\chi+\partial_\tau\tilde{n}\partial_\theta\chi)\}dD,$$

and

$$\mathrm{B}\langle[\sigma,\tilde{n}],[\upsilon,\chi]\rangle=\frac{\pi}{16}\int_D\omega\rho^3(\theta,\varphi)\sin\varphi\tilde{n}\upsilon dD.$$

We propose a Fourier-Legendre spectral-Galerkin method for (7), defining the basis functions

$$\Psi_k(\tau)=L_k(\tau)-L_{k+2}(\tau),\ \Phi_k(\varsigma)=L_k(\varsigma)-L_{k+2}(\varsigma),\ 0\le k\le N-2,\ \zeta_0(\tau)=1-\tau,$$

where L_k denotes the Legendre polynomial of degree k. These satisfy the essential boundary conditions:

$$\Psi_k(-1)=\Psi_k(1)=0,\Phi_k(-1)=\Phi_k(1)=0,\zeta_0(1)=0.$$

The approximation space $\mathbf{V}_{MNL}$ is then defined as

$$\mathbf{V}_{MNL}=\mathrm{V}_{MNL}\times\mathrm{V}_{MNL},$$

where

$$\mathrm{V}_{MNL}=\mathrm{span}\{\Psi_k(\tau)\Phi_l(\varsigma)\sin(m\theta),\Psi_k(\tau)\Phi_l(\varsigma)\cos(m\theta),$$
$$1\le m\le M,0\le k\le N-2,0\le l\le L-2\}\oplus\mathrm{span}\{\zeta_0\}$$
$$\oplus\mathrm{span}\{\Psi_k(\tau)L_l(\varsigma),0\le k\le N-2,0\le l\le L\}.$$

The Fourier-Legendre spectral-Galerkin approximation of (7) is then formulated as: Find $[\sigma_{MNL},\tilde{n}_{MNL}]\in\mathbf{V}_{MNL}$ such that for all $[\upsilon_{MNL},\chi_{MNL}]\in\mathbf{V}_{MNL}$,

$$\mathrm{A}\langle[\sigma_{MNL},\tilde{n}_{MNL}],[\upsilon_{MNL},\chi_{MNL}]\rangle=\hat{\lambda}\mathrm{B}\langle[\sigma_{MNL},\tilde{n}_{MNL}],[\upsilon_{MNL},\chi_{MNL}]\rangle. \tag{8}$$

III. EFFICIENT IMPLEMENTATION OF ALGORITHM

We develop an efficient numerical method for solving (8), beginning with expansions of the approximate solutions σ_{MNL} and $\tilde{n}_{MNL}$:

$$[\sigma_{MNL},\tilde{n}_{MNL}]=\Big[\sum_{k=0}^{N-2}\sum_{l=0}^{L-2}\sum_{m=1}^{M}(c^1_{klm}\Psi_k(\tau)\Phi_l(\varsigma)\sin(m\theta)+c^2_{klm}\Psi_k(\tau)\Phi_l(\varsigma)\cos(m\theta))$$
$$+c_3\zeta_0(\tau)+\sum_{k=0}^{N-2}\sum_{l=0}^{L}c^4_{kl}\Psi_k(\tau)L_l(\varsigma),\tilde{n}_3\zeta_0(\tau)+\sum_{k=0}^{N-2}\sum_{l=0}^{L}\tilde{n}^4_{kl}\Psi_k(\tau)L_l(\varsigma) \tag{9}$$
$$+\sum_{k=0}^{N-2}\sum_{l=0}^{L-2}\sum_{m=1}^{M}(\tilde{n}^1_{klm}\Psi_k(\tau)\Phi_l(\varsigma)\sin(m\theta)+\tilde{n}^2_{klm}\Psi_k(\tau)\Phi_l(\varsigma)\cos(m\theta))\Big].$$

Define the vector coefficients

Volume 9, Issue 12, pp. 66-75, 2025.
ISSN (Online): 2456-7361

$$\mathbf{w}_1=(c^1_{0,0,1},\cdots,c^1_{0,0,M},\cdots,c^1_{N-2,0,1},\cdots,c^1_{N-2,0,M},\cdots,c^1_{N-2,L-2,M})^{\bullet},$$
$$\mathbf{w}_2=(c^2_{0,0,1},\cdots,c^2_{0,0,M},\cdots,c^2_{N-2,0,1},\cdots,c^2_{N-2,0,M},\cdots,c^2_{N-2,L-2,M})^{\bullet},$$
$$\mathbf{w}_4=(c^4_{0,0},\cdots,c^4_{N-2,0},\cdots,c^4_{0,L},\cdots,c^4_{N-2,L})^{\bullet},$$
$$\mathbf{u}_1=(\tilde{n}^1_{0,0,1},\cdots,\tilde{n}^1_{0,0,M},\cdots,\tilde{n}^1_{N-2,0,1},\cdots,\tilde{n}^1_{N-2,0,M},\cdots,\tilde{n}^1_{N-2,L-2,M})^{\bullet},$$
$$\mathbf{u}_2=(\tilde{n}^2_{0,0,1},\cdots,\tilde{n}^2_{0,0,M},\cdots,\tilde{n}^2_{N-2,0,1},\cdots,\tilde{n}^2_{N-2,0,M},\cdots,\tilde{n}^2_{N-2,L-2,M})^{\bullet},$$
$$\mathbf{u}_4=(\tilde{n}^4_{0,0},\cdots,\tilde{n}^4_{N-2,0},\cdots,\tilde{n}^4_{0,L},\cdots,\tilde{n}^4_{N-2,L})^{\bullet},\mathbf{w}=(\mathbf{w}_1;\mathbf{w}_2;c_3;\mathbf{w}_4),\mathbf{u}=(\mathbf{u}_1;\mathbf{u}_2;\tilde{n}_3;\mathbf{u}_4).$$

We now introduce the element symbols as

$$_1a^{nm}_{lt}=\int_{\hat{D}}\hat{\eta}_1\Phi_l\sin(m\theta)\Phi_t\sin(n\theta)d\hat{D},{}_2a^{nm}_{lt}=\int_{\hat{D}}\hat{\eta}_2\Phi_l m\cos(m\theta)\Phi_t n\sin(n\theta)d\hat{D},$$
$$_3a^{nm}_{lt}=\int_{\hat{D}}\hat{\eta}_3\Phi'_l\sin(m\theta)\Phi'_t\sin(n\theta)d\hat{D},{}_4a^{m}_{lt}=\int_{\hat{D}}\hat{\eta}_4\Phi'_l\sin(m\theta)\Phi_t\sin(n\theta)d\hat{D},$$
$$_5a^{nm}_{lt}=\int_{\hat{D}}\hat{\eta}_4\Phi_l\sin(m\theta)\Phi'_t\sin(n\theta)d\hat{D},{}_6a^{nm}_{lt}=\int_{\hat{D}}\hat{\eta}_5\Phi_l m\cos(m\theta)\Phi_t n\sin(n\theta)d\hat{D},$$
$$_7a^{nm}_{lt}=\int_{\hat{D}}\hat{\eta}_5\Phi_l\sin(m\theta)\Phi_t n\cos(n\theta)d\hat{D},{}_8a^{m}_{lt}=\int_{\hat{D}}\hat{\eta}\Phi_l\sin(m\theta)\Phi_t\sin(n\theta)d\hat{D},$$
$$_1b^{nm}_{lt}=\int_{\hat{D}}\hat{\eta}_1\Phi_l\sin(m\theta)\Phi_t\cos(n\theta)d\hat{D},{}_2b^{nm}_{lt}=-\int_{\hat{D}}\hat{\eta}_2\Phi_l m\cos(m\theta)\Phi_t n\sin(n\theta)d\hat{D},$$
$$_3b^{nm}_{lt}=\int_{\hat{D}}\hat{\eta}_3\Phi'_l\sin(m\theta)\Phi'_t\cos(n\theta)d\hat{D},{}_4b^{m}_{lt}=\int_{\hat{D}}\hat{\eta}_4\Phi'_l\sin(m\theta)\Phi_t\cos(n\theta)d\hat{D},$$
$$_5b^{nm}_{lt}=\int_{\hat{D}}\hat{\eta}_4\Phi_l\sin(m\theta)\Phi'_t\cos(n\theta)d\hat{D},{}_6b^{nm}_{lt}=\int_{\hat{D}}\hat{\eta}_5\Phi_l m\cos(m\theta)\Phi_t n\cos(n\theta)d\hat{D},$$
$$_7b^{nm}_{lt}=\int_{\hat{D}}\hat{\eta}_5\Phi_l\sin(m\theta)\Phi_t n\cos(n\theta)d\hat{D},{}_8b^{m}_{lt}=\int_{\hat{D}}\hat{\eta}\Phi_l\sin(m\theta)\Phi_t\cos(n\theta)d\hat{D},$$
$$\hat{\eta}_1=\frac{\pi}{4}\omega p(\theta,\varphi),\hat{\eta}_2=\frac{\pi\rho(\theta,\varphi)}{4\sin\varphi},\hat{\eta}_3=\frac{1}{\pi}\rho(\theta,\varphi)\sin\varphi,\hat{\eta}_4=-\frac{1}{2}\partial_\varphi\rho(\theta,\varphi)\sin\varphi,$$
$$\hat{\eta}_5=-\frac{\pi\partial_\theta\rho(\theta,\varphi)}{4\sin\varphi},\hat{\eta}=\frac{\pi}{16}\rho^3(\theta,\varphi)\sin\varphi,\hat{D}=[0,\pi]\times[0,2\pi),$$

and

$$_1c^{nm}_{lt}=\int_{\hat{D}}\hat{\eta}_1\Phi_l\cos(m\theta)\Phi_t\sin(n\theta)d\hat{D},{}_2c^{nm}_{lt}=-\int_{\hat{D}}\hat{\eta}_2\Phi_l m\sin(m\theta)\Phi_t n\cos(n\theta)d\hat{D},$$
$$_3c^{nm}_{lt}=\int_{\hat{D}}\hat{\eta}_3\Phi'_l\sin(m\theta)\Phi'_t\sin(n\theta)d\hat{D},{}_4c^{m}_{lt}=\int_{\hat{D}}\hat{\eta}_4\Phi'_l\cos(m\theta)\Phi_t\sin(n\theta)d\hat{D},$$
$$_5c^{nm}_{lt}=\int_{\hat{D}}\hat{\eta}_4\Phi_l\cos(m\theta)\Phi'_t\sin(n\theta)d\hat{D},{}_6c^{nm}_{lt}=-\int_{\hat{D}}\hat{\eta}_2\Phi_l m\sin(m\theta)\Phi_t n\sin(n\theta)d\hat{D},$$
$$_7c^{nm}_{lt}=\int_{\hat{D}}\hat{\eta}_5\Phi_l\cos(m\theta)\Phi_t n\cos(n\theta)d\hat{D},{}_8c^{m}_{lt}=\int_{\hat{D}}\hat{\eta}\Phi_l\cos(m\theta)\Phi_t\sin(n\theta)d\hat{D},$$
$$_1d^{nm}_{lt}=\int_{\hat{D}}\hat{\eta}_1\Phi_l\cos(m\theta)\Phi_t\cos(n\theta)d\hat{D},{}_2d^{nm}_{lt}=-\int_{\hat{D}}\hat{\eta}_2\Phi_l m\sin(m\theta)\Phi_t n\sin(n\theta)d\hat{D},$$
$$_3d^{nm}_{lt}=\int_{\hat{D}}\hat{\eta}_3\Phi'_l\cos(m\theta)\Phi'_t\cos(n\theta)d\hat{D},{}_4d^{m}_{lt}=\int_{\hat{D}}\hat{\eta}_4\Phi'_l\cos(m\theta)\Phi_t\cos(n\theta)d\hat{D},$$
$$_5d^{nm}_{lt}=\int_{\hat{D}}\hat{\eta}_4\Phi_l\cos(m\theta)\Phi'_t\cos(n\theta)d\hat{D},{}_6d^{nm}_{lt}=-\int_{\hat{D}}\hat{\eta}_2\Phi_l m\sin(m\theta)\Phi_t n\cos(n\theta)d\hat{D},$$
$$_7d^{nm}_{lt}=-\int_{\hat{D}}\hat{\eta}_5\Phi_l\cos(m\theta)\Phi_t n\sin(n\theta)d\hat{D},{}_8d^{m}_{lt}=\int_{\hat{D}}\hat{\eta}\Phi_l\cos(m\theta)\Phi_t\cos(n\theta)d\hat{D}.$$

Moreover, we let

Volume 9, Issue 12, pp. 66-75, 2025. ISSN (Online): 2456-7361

$$_1e_l^m=\int_{\hat{D}}\hat{\eta}_1\Phi_l\sin(m\theta)d\hat{D},{}_2e_l^m=\int_{\hat{D}}\hat{\eta}_4\Phi_l^{'}\sin(m\theta)d\hat{D},{}_3e_l^m=\int_{\hat{D}}\hat{\eta}_5\Phi_l^{'}m\cos(m\theta)d\hat{D},$$

$$_4e_l^m=\int_{\hat{D}}\hat{\eta}_5\Phi_l\sin(m\theta)d\hat{D},{}_5e_l^m=\int_{\hat{D}}\hat{\eta}\Phi_l\sin(m\theta)d\hat{D},{}_1f_l^m=\int_{\hat{D}}\hat{\eta}_1\Phi_l\cos(m\theta)d\hat{D},$$

$$_2f_l^m=\int_{\hat{D}}\hat{\eta}_4\Phi_l^{'}\cos(m\theta)d\hat{D},{}_3f_l^m=-\int_{\hat{D}}\hat{\eta}_5\Phi_lm\sin(m\theta)d\hat{D},b_k^1=\int_\Lambda\omega\Psi_k^{'}\zeta_0^{'}d\tau,$$

$$_4f_l^m=\int_{\hat{D}}\hat{\eta}_5\Phi_l\cos(m\theta)d\hat{D},{}_5f_l^m=\int_{\hat{D}}\hat{\eta}\Phi_l\cos(m\theta)d\hat{D},b_k^2=\int_\Lambda(\tau+1)\Psi_k\zeta_0^{'}d\tau,$$

and

$$_1g_{lt}^m=\int_{\hat{D}}\hat{\eta}_1\Phi_l\sin(m\theta)L_td\hat{D},{}_2g_{lt}^m=\int_{\hat{D}}\hat{\eta}_3\Phi_l^{'}\sin(m\theta)L_t^{'}d\hat{D},{}_3g_{lt}^m=\int_{\hat{D}}\hat{\eta}_4\Phi_l^{'}\sin(m\theta)L_td\hat{D},$$

$$_4g_{lt}^m=\int_{\hat{D}}\hat{\eta}_4\Phi_l\sin(m\theta)L_t^{'}d\hat{D},{}_5g_{lt}^m=\int_{\hat{D}}\hat{\eta}_2\Phi_lm\cos(m\theta)L_td\hat{D},{}_6g_{lt}^m=\int_{\hat{D}}\hat{\eta}\Phi_l\sin(m\theta)L_td\hat{D},$$

$$_1h_{lt}^m=\int_{\hat{D}}\hat{\eta}_1\Phi_l\cos(m\theta)L_td\hat{D},{}_2h_{lt}^m=\int_{\hat{D}}\hat{\eta}_3\Phi_l^{'}\cos(m\theta)L_t^{'}d\hat{D},b_k^3=\int_\Lambda\omega\Psi_k\zeta_0d\tau,$$

$$_3h_{lt}^m=\int_{\hat{D}}\hat{\eta}_4\Phi_l^{'}\cos(m\theta)L_td\hat{D},{}_4h_{lt}^m=\int_{\hat{D}}\hat{\eta}_4\Phi_l\cos(m\theta)L_t^{'}d\hat{D},c_1=\frac{\pi}{4}\int_{\hat{D}}\hat{\eta}_1d\hat{D},$$

$$_5h_{lt}^m=-\int_{\hat{D}}\hat{\eta}_2\Phi_lm\sin(m\theta)L_td\hat{D},{}_6h_{lt}^m=\int_{\hat{D}}\hat{\eta}\Phi_l\cos(m\theta)L_td\hat{D},c_2=\frac{\pi}{16}\int_{\hat{D}}\hat{\eta}d\hat{D},$$

and

$$_1y_t^n=\int_{\hat{D}}\hat{\eta}_1\Phi_t\sin(n\theta)d\hat{D},{}_2y_t^n=\int_{\hat{D}}\hat{\eta}_4\Phi_t^{'}\sin(n\theta)d\hat{D},{}_3y_t^n=\int_{\hat{D}}\hat{\eta}_5\Phi_tn\cos(n\theta)d\hat{D},$$

$$_4y_t^n=\int_{\hat{D}}\hat{\eta}\Phi_t\sin(n\theta)d\hat{D},{}_1j_t^n=\int_{\hat{D}}\hat{\eta}_1\Phi_t\cos(n\theta)d\hat{D},{}_2j_t^n=\int_{\hat{D}}\hat{\eta}_4\Phi_t^{'}\cos(n\theta)d\hat{D},$$

$$_3j_t^n=-\int_{\hat{D}}\hat{\eta}_5\Phi_tn\sin(n\theta)d\hat{D},{}_4j_t^n=\int_{\hat{D}}\hat{\eta}\Phi_t\sin(n\theta)d\hat{D},d_j^1=\int_\Lambda\omega\Psi_j\zeta_0^{'}d\tau,$$

$$d_j^2=\int_\Lambda(\tau+1)\Psi_j\zeta_0^{'}d\tau,d_j^3=\int_\Lambda\omega\Psi_j\zeta_0d\tau,d_1=\int_\Lambda\omega\zeta_0^{'}\zeta_0^{'}d\tau,d_2=\int_\Lambda\omega\zeta_0\zeta_0d\tau,$$

$$_1l_{t1}=\frac{\pi}{4}\int_{\hat{D}}\hat{\eta}_1L_td\hat{D},{}_2l_{t1}=-\frac{1}{2}\int_{\hat{D}}\hat{\eta}_4L_t^{'}d\hat{D},{}_3l_{t1}=\frac{\pi}{16}\int_{\hat{D}}\hat{\eta}L_td\hat{D}.$$

We also denote

$$_1p_{lt}^n=\int_{\hat{D}}\hat{\eta}_1\Phi_t\sin(n\theta)L_ld\hat{D},{}_2p_{lt}^n=\int_{\hat{D}}\hat{\eta}_3\Phi_t^{'}\sin(n\theta)L_l^{'}d\hat{D},{}_3p_{lt}^n=\int_{\hat{D}}\hat{\eta}_4\Phi_t^{'}\sin(n\theta)L_ld\hat{D},$$

$$_4p_{lt}^n=\int_{\hat{D}}\hat{\eta}_4\Phi_t\sin(n\theta)L_l^{'}d\hat{D},{}_5p_{lt}^n=\int_{\hat{D}}\hat{\eta}_2\Phi_tn\cos(n\theta)L_ld\hat{D},{}_6p_{lt}^n=\int_{\hat{D}}\hat{\eta}\Phi_t\sin(n\theta)L_ld\hat{D},$$

$$_1q_{lt}^n=\int_{\hat{D}}\hat{\eta}_1\Phi_t\cos(n\theta)L_ld\hat{D},{}_2q_{lt}^n=\int_{\hat{D}}\hat{\eta}_3\Phi_t^{'}\cos(n\theta)L_l^{'}d\hat{D},{}_3q_{lt}^n=\int_{\hat{D}}\hat{\eta}_4\Phi_t^{'}\cos(n\theta)L_ld\hat{D},$$

$$_4q_{lt}^n=\int_{\hat{D}}\hat{\eta}_4\Phi_t\cos(n\theta)L_l^{'}d\hat{D},{}_5q_{lt}^n=-\int_{\hat{D}}\hat{\eta}_2\Phi_tn\sin(n\theta)L_ld\hat{D},{}_6q_{lt}^n=\int_{\hat{D}}\hat{\eta}\Phi_t\cos(n\theta)L_ld\hat{D},$$

and

$$_1o_{1l}=\int_{\hat{D}}\hat{\eta}_1L_ld\hat{D},{}_2o_{1l}=\int_{\hat{D}}\hat{\eta}_4L_l^{'}d\hat{D},{}_3o_{1l}=\int_{\hat{D}}\hat{\eta}L_ld\hat{D},{}_1s_{lt}=\int_{\hat{D}}\hat{\eta}_1L_tL_ld\hat{D},$$

$$_2s_{lt}=\int_{\hat{D}}\hat{\eta}_3L_t^{'}L_l^{'}d\hat{D},{}_3s_{lt}=\int_{\hat{D}}\hat{\eta}_4L_tL_l^{'}d\hat{D},{}_4s_{lt}=\int_{\hat{D}}\hat{\eta}_4L_t^{'}L_ld\hat{D},$$

$$_5s_{lt}=-\int_{\hat{D}}\hat{\eta}L_tL_ld\hat{D},a_{jk}^1=\int_\Lambda\omega\Psi_k^{'}\Psi_j^{'}d\tau,a_{jk}^2=\int_\Lambda\Psi_k\Psi_jd\tau,\Lambda=(-1,1),$$

$$a_{jk}^3=\int_\Lambda(\tau+1)\Psi_k^{'}\Psi_jd\tau,a_{jk}^4=\int_\Lambda(\tau+1)\Psi_k\Psi_j^{'}d\tau,a_{jk}^5=\int_\Lambda\omega\Psi_k\Psi_jd\tau.$$

Then, we define the matrices as follows:

International Journal of Scientific Engineering and Science
Volume 9, Issue 12, pp. 66-75, 2025. ISSN (Online): 2456-7361

$$A_1=({}_1a_{lt}^{nm}),\ A_2=({}_2a_{lt}^{nm}),\ A_3=({}_3a_{lt}^{nm}),\ A_4=({}_4a_{lt}^{nm}),\ A_5=({}_5a_{lt}^{nm}),$$
$$A_6=({}_6a_{lt}^{nm}),\ A_7=({}_7a_{lt}^{nm}),\ A_8=({}_8a_{lt}^{nm}),\ B_1=({}_1b_{lt}^{nm}),\ B_2=({}_2b_{lt}^{nm}),$$
$$B_3=({}_3b_{lt}^{nm}),\ B_4=({}_4b_{lt}^{nm}),\ B_5=({}_5b_{lt}^{nm}),\ B_6=({}_6b_{lt}^{nm}),\ B_7=({}_7b_{lt}^{nm}),$$
$$B_8=({}_8b_{lt}^{nm}),\ C_1=({}_1c_{lt}^{nm}),\ C_2=({}_2c_{lt}^{nm}),\ C_3=({}_3c_{lt}^{nm}),\ C_4=({}_4c_{lt}^{nm}),$$
$$C_5=({}_5c_{lt}^{nm}),\ C_6=({}_6c_{lt}^{nm}),\ C_7=({}_7c_{lt}^{nm}),\ C_8=({}_8c_{lt}^{nm}),\ D_1=({}_1d_{lt}^{nm}),$$
$$D_2=({}_2d_{lt}^{nm}),\ D_3=({}_3d_{lt}^{nm}),\ D_4=({}_4d_{lt}^{nm}),\ D_5=({}_5d_{lt}^{nm}),\ D_6=({}_6d_{lt}^{nm}),$$
$$D_7=({}_7d_{lt}^{nm}),\ D_8=({}_8d_{lt}^{nm}),\ E_1=({}_1e_l^{m}),\ E_2=({}_2e_l^{m}),\ E_3=({}_3e_l^{m}),$$
$$E_4=({}_4e_l^{m}),\ E_5=({}_5e_l^{m}),\ F_1=({}_1e_l^{m}),\ F_2=({}_2e_l^{m}),\ F_3=({}_3e_l^{m}),$$
$$F_4=({}_4e_l^{m}),\ F_5=({}_5e_l^{m}),\ O_1=({}_1o_{1l}),\ O_2=({}_2o_{1l}),\ O_3=({}_3o_{1l}),$$
and
$$G_1=({}_1g_{lt}^{m}),\ G_2=({}_2g_{lt}^{m}),\ G_3=({}_3g_{lt}^{m}),\ G_4=({}_4g_{lt}^{m}),\ G_5=({}_5g_{lt}^{m}),G_6=({}_6g_{lt}^{m}),$$
$$G_7=({}_7g_{lt}^{m}),\ G_8=({}_8g_{lt}^{m}),\ H_1=({}_1h_{lt}^{m}),\ H_2=({}_2h_{lt}^{m}),\ H_3=({}_3h_{lt}^{m}),\ H_4=({}_4h_{lt}^{m}),$$
$$H_5=({}_5h_{lt}^{m}),\ H_6=({}_6h_{lt}^{m}),\ H_7=({}_7h_{lt}^{m}),\ H_8=({}_8h_{lt}^{m}),\ Y_1=({}_1y_t^{n}),Y_2=({}_2y_t^{n}),$$
$$Y_3=({}_3y_t^{n}),\ Y_4=({}_4y_t^{n}),\ J_1=({}_1j_t^{n}),\ J_2=({}_2j_t^{n}),\ J_3=({}_3j_t^{n}),\ J_4=({}_4j_t^{n}),$$
$$P_1=({}_1p_{lt}^{n}),\ P_2=({}_2p_{lt}^{n}),\ P_3=({}_3p_{lt}^{n}),\ P_4=({}_4p_{lt}^{n}),\ P_5=({}_5p_{lt}^{n}),\ P_6=({}_6p_{lt}^{n}),$$
$$Q_1=({}_1q_{lt}^{n}),\ Q_2=({}_2q_{lt}^{n}),\ Q_3=({}_3q_{lt}^{n}),\ Q_4=({}_4q_{lt}^{n}),\ Q_5=({}_5q_{lt}^{n}),\ Q_6=({}_6q_{lt}^{n}),$$
$$S_1=({}_1s_{lt}),\ S_2=({}_2s_{lt}),\ S_3=({}_3s_{lt}),\ S_4=({}_4s_{lt}),\ S_5=({}_5s_{lt}),\ L_1=({}_1l_{t1}),$$
$$\mathbf{A}_1=(a_{jk}^1),\ \mathbf{A}_2=(a_{jk}^2),\ \mathbf{A}_3=(a_{jk}^3),\ \mathbf{A}_4=(a_{jk}^4),\ \mathbf{A}_5=(a_{jk}^5),\ L_2=({}_2l_{t1}),$$
$$\mathbf{B}_1=(b_k^1),\ \mathbf{B}_2=(b_k^2),\ \mathbf{B}_3=(b_k^3),\ \mathbf{D}_1=(d_j^1),\ \mathbf{D}_2=(d_j^2),\ \mathbf{D}_3=(d_j^3),\ L_3=({}_3l_{t1}).$$

Plugging (9) into (8) and taking $[\upsilon_{MNL},\chi_{MNL}]$ through all the basis functions in $\mathbf{V}_{MNL}$, we can derive the compact matrix form of (8) as follows:

$$\begin{bmatrix}\mathrm{A}+\alpha\mathrm{B} & \mathrm{B}\\ -\mathrm{B} & \mathrm{A}\end{bmatrix}\begin{bmatrix}\mathbf{w}\\ \mathbf{u}\end{bmatrix}=\hat{\lambda}_{MNL}\begin{bmatrix}\mathbf{0} & \mathrm{B}\\ \mathbf{0} & \mathbf{0}\end{bmatrix} \qquad (10)$$

with

$$\mathrm{A}=\begin{bmatrix}\mathrm{A}_1 & \mathrm{B}_1 & \square_1 & \mathrm{D}_1\\ \mathrm{A}_2 & \mathrm{B}_2 & \square_2 & \mathrm{D}_2\\ \mathrm{A}_3 & \mathrm{B}_3 & \square_3 & \mathrm{D}_3\\ \mathrm{A}_4 & \mathrm{B}_4 & \square_4 & \mathrm{D}_4\end{bmatrix},\qquad \mathrm{B}=\begin{bmatrix}\mathrm{A}_1 & \mathrm{B}_1 & \square_1 & \mathrm{D}_1\\ \mathrm{A}_2 & \mathrm{B}_2 & \square_2 & \mathrm{D}_2\\ \mathrm{A}_3 & \mathrm{B}_3 & \square_3 & \mathrm{D}_3\\ \mathrm{A}_4 & \mathrm{B}_4 & \square_4 & \mathrm{D}_4\end{bmatrix},$$

where

$$\mathrm{A}_1=A_1\otimes\mathbf{A}_1+A_2\otimes\mathbf{A}_2+A_3\otimes\mathbf{A}_2+A_4\otimes\mathbf{A}_3+A_5\otimes\mathbf{A}_4+A_6\otimes\mathbf{A}_3+A_7\otimes\mathbf{A}_4,$$
$$\mathrm{A}_2=B_1\otimes\mathbf{A}_1+B_2\otimes\mathbf{A}_2+B_3\otimes\mathbf{A}_2+B_4\otimes\mathbf{A}_3+B_5\otimes\mathbf{A}_4+B_6\otimes\mathbf{A}_3+B_7\otimes\mathbf{A}_4,$$
$$\mathrm{A}_3=E_1\otimes\mathbf{B}_1+E_2\otimes\mathbf{B}_2+E_3\otimes\mathbf{B}_2,\ \mathrm{A}_3=E_4\otimes\mathbf{B}_3,$$
$$\mathrm{A}_4=G_1\otimes\mathbf{A}_1+G_2\otimes\mathbf{A}_2+G_3\otimes\mathbf{A}_3+G_4\otimes\mathbf{A}_3+G_5\otimes\mathbf{A}_4+G_6\otimes\mathbf{A}_5,$$
$$\mathrm{B}_1=C_1\otimes\mathbf{A}_1+C_2\otimes\mathbf{A}_2+C_3\otimes\mathbf{A}_2+C_4\otimes\mathbf{A}_3+C_5\otimes\mathbf{A}_4+C_6\otimes\mathbf{A}_3+C_7\otimes\mathbf{A}_4,$$
$$\mathrm{B}_2=D_1\otimes\mathbf{A}_1+D_2\otimes\mathbf{A}_2+C_3\otimes\mathbf{A}_2+D_4\otimes\mathbf{A}_3+D_5\otimes\mathbf{A}_4+D_6\otimes\mathbf{A}_3+D_7\otimes\mathbf{A}_4,$$

$$\mathrm{B}_3 = F_1 \otimes \mathbf{B}_1 + F_2 \otimes \mathbf{B}_2 + F_3 \otimes \mathbf{B}_2 + F_4 \otimes \mathbf{B}_3, \mathrm{B}_3 = F_4 \otimes \mathbf{B}_3,$$
$$\mathrm{B}_4 = H_1 \otimes \mathbf{A}_1 + H_2 \otimes \mathrm{A}_2 + H_3 \otimes \mathbf{A}_3 + H_4 \otimes \mathbf{A}_3 + H_5 \otimes \mathbf{A}_4 + H_6 \otimes \mathbf{A}_5,$$
$$\square_1 = Y_1 \otimes \mathbf{D}_1 + Y_2 \otimes \mathbf{D}_2 + Y_3 \otimes \mathbf{D}_2, \square_2 = J_1 \otimes \mathbf{D}_1 + J_2 \otimes \mathbf{D}_2 + J_3 \otimes \mathbf{D}_2,$$
$$\square_3 = c_1 d_1, \square_4 = L_1 \otimes \mathbf{D}_1 + L_2 \otimes \mathbf{D}_2, \square_1 = Y_4 \otimes \mathbf{D}_3, \square_2 = J_4 \otimes \mathbf{D}_3,$$
$$\mathrm{D}_1 = P_1 \otimes \mathbf{A}_1 + P_2 \otimes \mathbf{A}_2 + P_3 \otimes \mathbf{A}_3 + P_4 \otimes \mathbf{A}_3 + P_5 \otimes \mathbf{A}_4,$$
$$\mathrm{D}_2 = Q_1 \otimes \mathbf{A}_1 + Q_2 \otimes \mathbf{A}_2 + Q_3 \otimes \mathbf{A}_3 + Q_4 \otimes \mathbf{A}_3 + Q_5 \otimes \mathbf{A}_4,$$
$$\mathrm{D}_3 = O_1 \otimes \mathbf{B}_1 + O_2 \otimes \mathbf{B}_2, \mathrm{D}_4 = S_1 \otimes \mathbf{A}_1 + S_2 \otimes \mathbf{A}_2 + S_3 \otimes \mathbf{A}_3 + S_4 \otimes \mathbf{A}_4,$$

and

$$\mathrm{A}_1 = A_8 \otimes \mathbf{A}_5, \mathrm{A}_2 = B_8 \otimes \mathbf{A}_5, \mathrm{B}_1 = C_8 \otimes \mathbf{A}_5, \mathrm{B}_2 = D_8 \otimes \mathbf{A}_5,$$
$$\mathrm{A}_4 = G_8 \otimes \mathbf{A}_5, \mathrm{B}_4 = H_8 \otimes \mathbf{A}_5, \square_3 = c_2 d_2, \square_4 = L_3 \otimes \mathbf{D}_3,$$
$$\mathrm{D}_1 = P_6 \otimes \mathbf{A}_5, \mathrm{D}_2 = Q_6 \otimes \mathbf{A}_5, \mathrm{D}_3 = O_3 \otimes \mathbf{B}_3, \mathrm{D}_4 = S_5 \otimes \mathbf{A}_5.$$

IV. NUMERICAL SIMULATION

In this section, a series of numerical experiments are presented for the problem (1) on three-dimensional domains to exhibit the performance of the proposed method. Our program is compiled and executed in MATLAB R2021a.

Example 1: We take $\alpha = \beta = 1$, and consider the ellipsoidal domain Ω (see Figure 1), that is

$$\rho(\theta,\varphi) = \left(\frac{\cos^2\theta\sin^2\varphi}{4} + \frac{\sin^2\theta\sin^2\varphi}{4} + \frac{\cos^2\varphi}{16}\right)^{-\frac{1}{2}}.$$

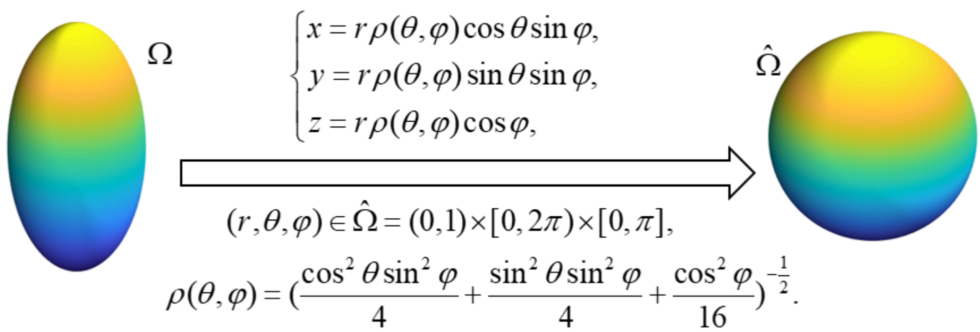

Fig.1 Original region Ω (left) and its mapped counterpart $\hat{\Omega}$ (right).

The numerical results of the four eigenvalues $\lambda^1_{MNL}, \lambda^2_{MNL}, \lambda^3_{MNL}$ and λ^4_{MNL} for different L, N, M are listed in Tables 1-3, respectively. In order to show convergence and spectral accuracy of the algorithm, we choose the numerical solution with $M = 12$, $N = 16, L = 30$ as the reference solution, and plot the error curves of approximate eigenvalues in Figure 2. To further illustrate the convergence of the approximation function, we also provide the corresponding error curves under the L^2 - norm with different N, L in Figure 3.

Tab.1 Numerical results of the first four approximation eigenvalues for different L with $M = 12, N = 16$.

L	λ^1_{MNL}	λ^2_{MNL}	λ^3_{MNL}	λ^4_{MNL}
10	6.137164813311033	10.92532863437599	19.23695565813545	23.06366680052173
15	6.137091336276788	10.92297299707570	19.22195665028664	23.06442461934928
20	6.137091046702165	10.92297073107012	19.22188392192395	23.06442324359357
25	6.137091047052889	10.92297073208283	19.22188394805047	23.06442323723938

Tab.2 Numerical results of the first four approximation eigenvalues for different N with $M=12, L=30$.

N	λ^1_{MNL}	λ^2_{MNL}	λ^3_{MNL}	λ^4_{MNL}
6	6.137091340705462	10.92301634400544	19.22279187152741	23.06450107279335
8	6.137091047158824	10.92297077355707	19.22188597654588	23.06442332365593
10	6.137091047054016	10.92297073218531	19.22188395054466	23.06442323722825
12	6.137091047053985	10.92297073216803	19.22188394858740	23.06442323717651

Tab.3 Numerical results of the first four approximation eigenvalues for different M with $N=16, L=30$.

M	λ^1_{MNL}	λ^2_{MNL}	λ^3_{MNL}	λ^4_{MNL}
2	6.137091047053993	10.92297073216801	19.22188394858636	23.06442323717633
4	6.137091047053995	10.92297073216801	19.22188394858637	23.06442323717638
6	6.137091047054005	10.92297073216799	19.22188394858630	23.06442323717629
8	6.137091047053983	10.92297073216798	19.22188394858638	23.06442323717629

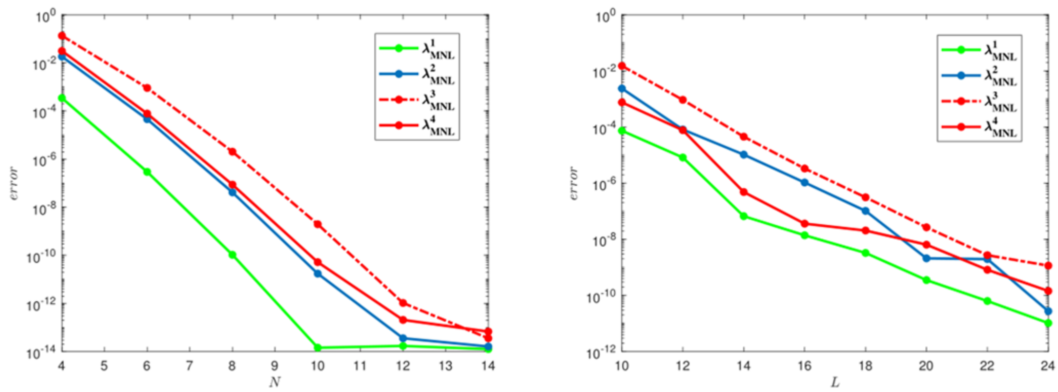

Fig.2 Error curves between approximation solutions and reference solution for varying N (left) and L (right).

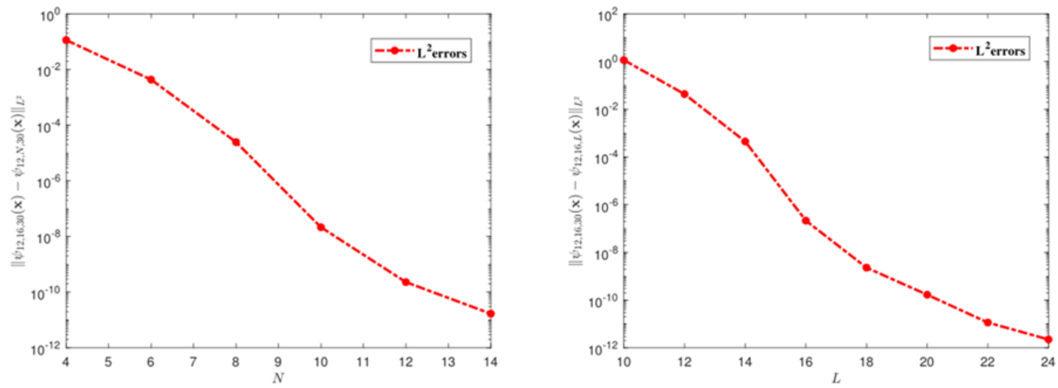

Fig.3 Error curves between approximation solutions and reference solution for varying N (left) and L (right).

As shown in Tables 1-3, when $N \geq 12, M \geq 8$, and $L \geq 25$, the eigenvalues achieve at least 11-digit precision. Furthermore, Figures 2-3 corroborate the algorithm's convergence and spectral accuracy.

V. CONCLUSION

In this paper, we present an efficient spectral method based on a hybrid formulation for solving fourth-order eigenvalue problems in ellipsoidal domains. By employing spherical coordinates, we map the ellipsoidal region onto a regular unit sphere domain, establishing the weak form and its corresponding discrete variational formulation within the transformed domain. Furthermore, the algorithm's validity and high accuracy are verified through numerical validation. In addition, the algorithm proposed in this paper can be extended to more complex nonlinear problems, such as the Cahn–Hilliard equation, which is our next research goal.

International Journal of Scientific Engineering and Science
Volume 9, Issue 12, pp. 66-75, 2025. ISSN (Online): 2456-7361

REFERENCES

[1] J. An, H. Li, Z. Zhang. Spectral-Galerkin approximation and optimal error estimate for biharmonic eigenvalue problems in circular/spherical/elliptical domains. Numer. Algor., 2020, 84(2): 427-455.
[2] C. Canuto, M.Y. Hussaini, A. Quarteroni, T.A. Zang. Spectral Methods. Fundamentals in Single Domains. Springer-Verlag, Berlin, 2006.
[3] C. Canuto, M.Y. Hussaini, A. Quarteroni, T.A. Zang. Spectral Methods. Evolution to Complex Geometries and Applications to Fluid Dynamics. Springer-Verlag, Berlin, 2007.
[4] D. Gottlieb, S.A. Orszag. Numerical Analysis of Spectral Methods: Theory and Applicaitions. SIAMCBMS, Philadelphia, 1977.
[5] B. Y. Guo. Spectral Methods and their Applications. World Scientific, Singapore, 1998.
[6] J. Shen, T. Tang, L. L. Wang. Spectral Methods: Algorithms, Analysis and Applica -tions. Springer-Verlag, Berlin, 2011.
[7] X. M. Xiang, Z.Q. Wang. Generalized Hermite spectral method and its applications to problems in unbounded domains. SIAM J. Numer. Anal., 2010. 48: 1231-1253.
[8] L. J. Yi, B. Q. Guo. An h−p version of the continuous Petrov-Galerkin finite element method for Volterra integro-differential equations with smooth and nonsmooth kernels.SIAM J. Numer. Anal., 2015, 53: 2677-2704.
[9] K. Z. Korczak, A.T. Patera. An isoparametric spectral element method for solution of the Navier-Stokes equations in complex geometry. J. Comput. Phys., 1986, 62:361-382.
[10] L. F. Pavarino, O.B. Widlund, S. Zampini. BDDC preconditioners for spectral element discretizations of almost incompressible elasticity in three dimensions. SIAM J. Sci. Comput., 2010, 32: 3604-3626.
[11] A. Quarteroni, A. Valli. Domain Decomposition Methods for Partial Differential E-quations. Oxford University Press, Oxford, 1999.
[12] J. Shen. Efficient spectral-Galerkin methods. IV. Spherical geometries. SIAM J. Sci. Comput., 1999, 20: 1438-1455.
[13] J. Shen, L. L. Wang, H.Y. Li. A triangular spectral element method using fully tensorial rational basis functions. SIAM J. Numer. Anal., 2009, 47: 1619-1650.
[14] F. Y. Song, C.J. Xu, G. E. Karniadakis. Computing fractional Laplacians on complex-geometry domains: algorithms and simulations. SIAM J. Sci. Comput., 2017, 39:A1320-A1344.
[15] A. Toselli, O. Widlund. Domain Decomposition Methods-Algorithms and Theory.Springer-Verlag, Berlin, 2005.
[16] D. Furihata. A stable and conservative finite difference scheme for the Cahn-Hilliard equation, Numer. Math., 2001, 87: 675-699.
[17] H.G. Lee, J.S. Lowengrub, J. Goodman. Modeling pinchoff and reconnection in a Hele-Shaw cell. II. Analysis and simulation in the nonlinear regime. Phys. Fluids, 2002, 14:514-545.
[18] C. Liu, J. Shen. A phase-field model for the mixture of two incompressible fluids and its approximation by a Fourier-spectral method. Physica D, 2003, 179: 211-228.
[19] G. Dziuk, C.M. Elliot. Finite element methods for surface PDEs. Acta Numer., 2013, 22: 289-396.
[20] S. Zhao, X. Xiao, X. Feng. An efficient time adaptively based on chemical potential for surface Cahn-Hilliard equation using finite element approximation. Appl. Math. Comput., 2020, 369: 124901.
[21] Q. Du, L. Ju, L. Tian. Finite element approximation for the Cahn-Hilliard equation on surface Comput. Methods Appl. Mech. Engrg., 2011, 200: 2458-2470.
[22] D. Marenduzzo, E. Orlandini. Phase separation dynamics on curved surfaces. Soft Matter, 2013, 9: 1178-1187.
[23] B.L. Buzbee, F.W.Dorr, J.A. George, G.H.Golub. The direct solution of the discrete Poisson equation on irregular regions. SIAM J. Numer. Anal., 1971, 8: 722-736.
[24] S.A. Orszag. Spectral methods for problems in complex geometries. J. Comput. Phys., 1980, 37: 70-92.
[25] W. J. Gordon, C. A. Hall. Transfinite element methods: Blending-function interpola-tion over arbitrary curved element domains. Numer. Math., 1973, 21: 109-129.
[26] S. H. Lui. Spectral domain embedding for elliptic PDEs in complex domains. J. Comput. Appl. Math., 2009, 225: 541-557.
[27] Y. Q. Gu, J. Shen. Accurate and efficient spectral methods for elliptic PDEs in complex domains. J. Sci. Comput., 2020, 83: 42.
[28] Y. Q. Gu, J. Shen. An efficient spectral method for elliptic PDEs in complex domains with circular embedding. SIAM J. Sci. Comput., 2021, 43: A309-A329.
[29] Z.Q. Wang, X. Wen, G. Q. Yao. An efficient spectral-Galerkin method for elliptic equations in 2D complex geometries. J. Sci. Comput., 2023, 95(3): 89.
[30] G. Q. Yao, X. Wen, Z.Q. Wang. Efficient spectral methods for PDEs in three dimensional curved geometries. J. Sci. Comput., 2025, 103(3): 95.